ISSN 1028-334X, Doklady Earth Sciences, 2022, Vol. 506, Suppl. 1, pp. S48–S54. © Pleiades Publishing, Ltd., 2022.

GEOMORPHOLOGY

Fluctuations of Nero Lake in the Holocene

E. A. Konstantinov[a,*], N. V. Karpukhina[a], A. L. Zakharov[a], S. S. Bricheva[a,b], V. Yu. Ukraintsev[a], L. I. Lazukova[a], and A. I. Rudinskaya[a]

Received April 1, 2022; revised June 25, 2022; accepted June 30, 2022

Abstract—The paleohydrological settings in the Rostov lowland (Yaroslavl oblast) have been the subject of long-standing of disputes. The concepts for the Holocene fluctuations in the level of Nero Lake differ considerably among researchers. We have studied the structure of bottom sediments and bottom relief in the deepest, northeastern, part of the lake. A bathymetric survey was carried out. Drilling with the selection of undisturbed columns, GPR profiling, radiocarbon dating, and lithological analyses were conducted. Stratigraphic unconformities in the structure of the bottom sediments indicate a drop in the lake level in the Late Glacial and Early Holocene. The level dropped to 87 m asl, which is 7 m lower than the current water level in the lake. The size of the lake at this stage was reduced several times. The transgressive stage was established from 9 to 6.5 ka B.P.: the mean annual level of the lake could have risen up to 91–94 m asl, which is close to the modern level. In the interval from 6.5 to 2.4 ka B.P., a decrease in the level by 1–3 m below the current level is revealed. Then the level begins to grow gradually until it reached the current values 300–500 years ago. The main factor in the fluctuations in the level of Nero Lake in the Holocene is the change in the height of runoff threshold, caused by vertical deformations of the Ustye, Veksa, and Kotorosl river systems. These deformations were associated both with regional changes in fluvial activity and with the self-development of river channels.

Keywords: paleolimnology, lacustrine deposits, facies analysis, hiatuses, Rostov lowland

DOI: 10.1134/S1028334X22700258

INTRODUCTION

Shallow Nero Lake is located within the Rostov lowland about 180 km northeast of Moscow. This object has attracted the attention of geologists and paleogeographers studying the Quaternary period for over a century. There are several reasons for such interest. First, the large thickness (more than 70 m [9]) of the Late Pleistocene and Holocene lacustrine deposits makes this object attractive as a comprehensive archive of paleogeographic information. Second, the presence of a well-defined complex of terraces on the coast allows us to use them as reference levels for reconstruction of ancient lake basins. Third, a large number of archaeological monuments of a wide chronological range, from the Neolithic to the Middle Ages, is known in the Rostov depression [1].

Despite the long history of more than a century of the study of Nero Lake [3], there are still many controversial questions concerning the amplitude and age of fluctuations of the lake level in the past, as well as the causes of these fluctuations. Thus, high terraces on the sides of the Rostov lowland were considered by D.D. Kvasov [6] as Late Valdai. According to his ideas, the level of Nero Lake at the end of the Late Pleistocene rose to 145 m asl and the lake itself had a connection with a system of glacial water bodies. According to V.S. Gunova [4], the level of Nero Lake in the Late Valdai did not exceed 110 m asl, high terrasses were dated as the Late Moscovian.

The Holocene history of Nero Lake is no less discussible. Thus, according to the data of A.L. Alexandrovsky [1] and V. S. Gunova and O. N. Leflat [5], the lake level could have exceeded the modern one at the end of the Late Glacial and Early Holocene. However, the results of B. Wohlfarth [14], on the contrary, indicate an regressive level of the lake in the Early Holocene. V.Yu. Lavrushin [7] reconstructed a significant rise in the water level in the Nero–Kotorosl–Timirevo system with the formation of a single water body during the medieval climatic optimum. In other works, this large medieval transgression is not recorded. There is an agreement in explaining the causes of the level fluctuations. All of the above researchers relate them to the degree of climate humidity: more arid stages correspond to a low level, and more humid stages relate to a high level.

Analysis of the literature has shown that a significant part of the contradictions in the hydrological his-

[a] *Institute of Geography, Russian Academy of Sciences, Moscow, 119017 Russia*
[b] *Moscow State University, Moscow, 119991 Russia*
**e-mail: eakonst@igras.ru*

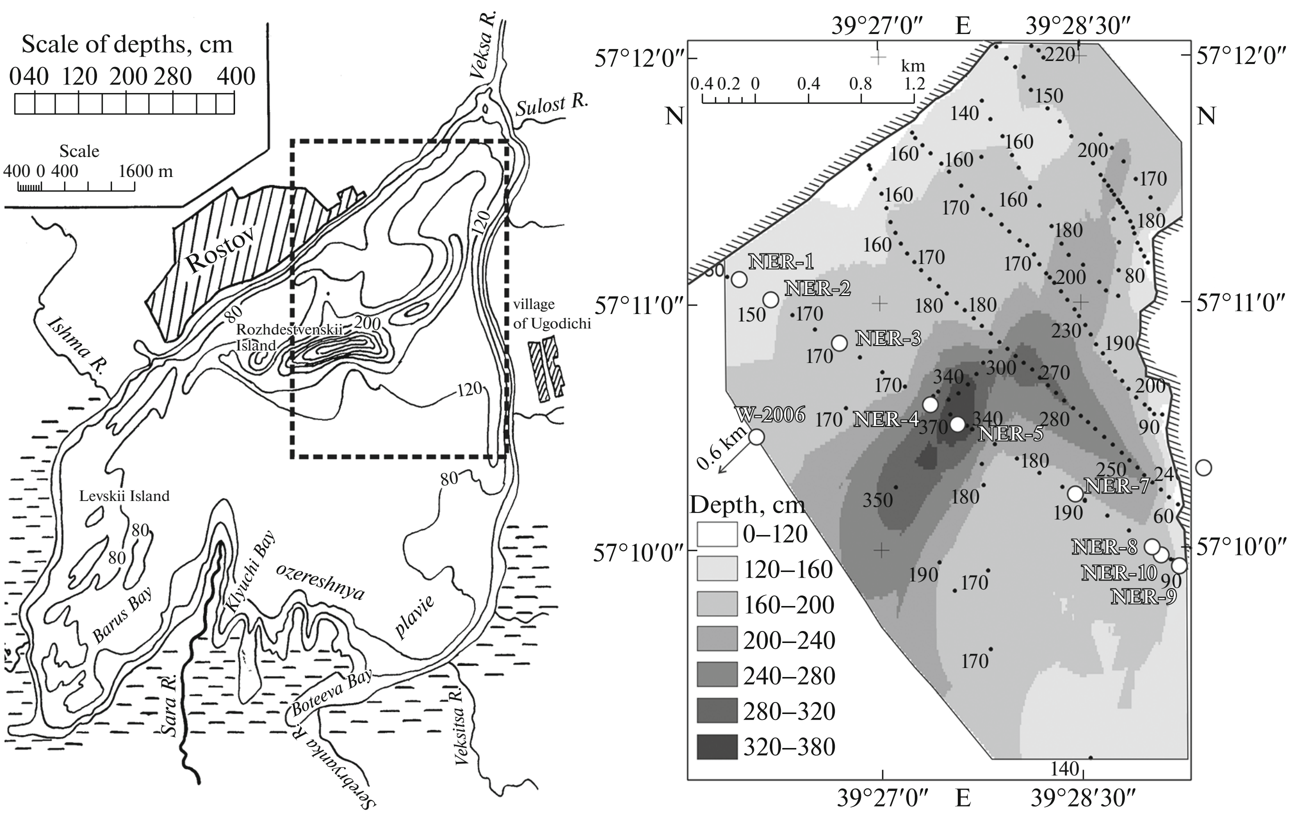

Fig. 1. The distribution of depths in Nero Lake: a, bathymetric scheme (according to [2]); b, bathymetric map of the northeastern part of the water area, compiled from results of measurements in winter 2020. Designations on the figure (b): black points are the depths at the sites of measuring, cm; white circles are boreholes; boreholes with the NER index are the author's results; and the W-2006 borehole is from the work by [14].

tory of Nero Lake have developed because cores of the bottom sediments and terraces are poorly dated and are not well studied in terms of lithology. In addition, there is no reliable bathymetric map.

This work attempts to fill the above gaps in part. The suggested curve of the level fluctuations of Nero Lake in the Holocene is based on the results of our studies of the structure of the bottom relief and sediments, stratigraphic unconformities, and on radiocarbon dating and lithological analyses; we also consider the previous reconstructions.

METHODS

In February 2020, depth measurements were made from ice in the northeastern part of the lake. The height of the water level of the lake, relative to which the depth measurements were taken, was recorded by the EFT M4 GNSS rover in the Real Time Kinematic (RTK) mode. The water level was 94.2 m (according to EGM08 geoid). In total, the depths were measured at 180 points, and the covered area was 14.7 km^2. The bathymetric map (Fig. 1) was compiled in ArcMap 10.3 on the basis of measurements interpolated by the ordinary kriging method (spherical model).

Using the Livingstone piston corer, nine boreholes were drilled from ice along the Rostov–Ugodichi profile (Fig. 1). Along the profile, a ground-penetrating radar (GPR) survey was carried out with the "Zond 12e" radar with a 300 MHz antenna and a Python3 radar with 100 MHz antenna. The laboratory studies were performed at the Laboratory of the environmental paleoarchives of the Institute of Geography RAS for samples from two cores (NER-3 and NER-5). Loss on ignition (LOI) in two temperature regimes (550 and 950°C), the magnetic susceptibility, and the particle-size distribution were determined. The $CaCO_3$ content (carbonate content) was calculated on the basis of LOI results according to the procedure [11]. Six radiocarbon dates were obtained from the NER-5 core samples by the accelerator mass spectrometry (AMS) method, and one date was obtained by the scintillation method (Table 1). AMS dating was performed in the laboratory of radiocarbon dating and electron microscopy of the Institute of Geography, Russian Academy of Sciences, jointly with the Center for Isotope Studies of the University of Georgia

Table 1. Results of radiocarbon dating of the samples from the NER-5 core

Lab. number	Column	Depth, m	Material, dating fraction	Method	^{14}C date, years ago	Cal. age B.P. (average ± 1 sigma)
IGAN8253	NER-5	0.75	Organo-mineral silt, total org. carbon	AMS	4855 ± 20	5580 ± 30
LU-9517	NER-5	0.85–1.0	Organo-mineral silt, total org. carbon	Scintill. method	5640 ± 190	6460 ± 220
IGAN8254	NER-5	2.35	Terrigenous-carbonate silt with admixture of org. matter, total org. carbon	AMS	6430 ± 25	7360 ± 40
IGAN8255	NER-5	3.75	Terrigenous-carbonate silt with admixture of org. matter, total org. carbon	AMS	7300 ± 25	8100 ± 40
IGAN 6783	NER-5	5.38	Terrigenous-carbonate silt with admixture of org. matter, total org. carbon	AMS	8215 ± 25	9180 ± 60
IGAN 6784	NER-5	7.18	Terrigenous-carbonate silt with admixture of org. matter, total org. carbon	AMS	9190 ± 30	10340 ± 60
IGAN 6785	NER-5	8.6	Terrigenous-carbonate silt with admixture of org. matter, total org. carbon	AMS	9900 ± 30	11290 ± 40

(United States). The scintillation date was obtained at the radiocarbon laboratory of St. Petersburg State University. Construction of the age models of sedimentation for the NER-5 and W-2006 cores (according to the dates from [14]) was performed on the basis of radiocarbon dating by the Bayesian method in the package Bacon v.2.4.0. environment R. Calibration of the radiocarbon dates was performed in the application OxCal Online using an IntCal20 calibration curve.

RESULTS

The distribution of the depths, presented on the bathymetric map (Fig. 1), allows us to detail significantly the conceptions about the bottom relief of the northeastern part of the water area of Nero Lake. Thus, it was revealed that the deep trough has a northeastern orientation. The dimensions and shape of the trough have been clarified. Its width varies from 400 to 800 m, and its length is up to 2.5–3.0 km. The maximum depth is up to 3.8 m in the area of the NER-5 borehole. The transverse U-shape profile of the trough has very gentle sides. The longitudinal profile is wavy with a manifested depression in the central part. The trough branches to the northeast of the drilling profile. The trough gradually flattens out towards the Veksa River head and becomes poorly manifested in the bottom relief. The deeper branch of the trough makes a knee-shaped bend in the southeastern direction, towards the village of Ugodichi. Outside the troughs, the bottom of the lake is represented by homogeneous shallows with depths of 1.2–1.8 m. The underwater coastal slopes are usually very gentle.

Drilling results showed that the upper part of the sediment (layer 1 in Fig. 2) is represented by poorly consolidated organo-mineral silt (suspended matter) up to 1.0 m thick. The presence of this layer does not always allow us to determine unambiguously the boundary between the water and the bottom because of the smooth transition to the dense sediment. This was probably one of the reasons for the indistinct reflected signal from the bottom surface on the obtained radargram.

Below, the sediment is represented by shaped dark gray organo-mineral silt (layer 2) 0.5–2.5 m thick. The minimum thickness of this layer is observed in the deep part of the axial trough. According to the LOI data, the organic matter content in this layer varies from 18 to 45%, and the carbonate content ranges from 6 to 30%. In the grain size composition of the silicate part of the sediment, the silty fraction (5–50 μm) dominates varying from 62 to 76%. The sand content (50–1000 μm) varies from 8 to 23%, and the clay content (<5 μm) ranges from 10 to 16%. The magnetic susceptibility is characterized by extremely low values, about 0.01×10^{-3} SI. According to the age models, the age of formation of layer 2 is between 6.5 and 0.5 cal ka B.P. Organo-mineral silt is found almost everywhere, except for the shallow coastal waters. The silt is underlain by more dense light olive terrigenous–carbonate

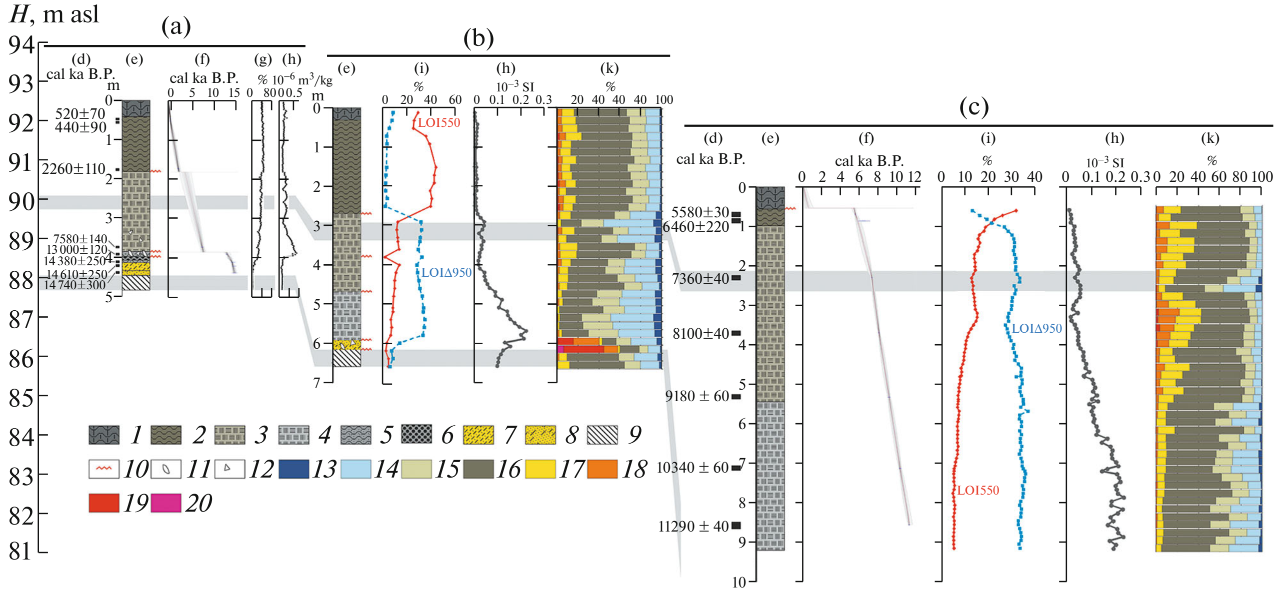

Fig. 2. The correlation scheme of the reference columns of bottom sediments. Letter designations: a, W-2006 core (from [14]); b, NER-3 core; c, NER-5 core; d, calibrated radiocarbon dates; e, lithological columns; f, age models; g, water content; h, magnetic susceptibility; i, losses on ignition; k, particle size distribution. Legend to the columns: *1*, poorly consolidated silt; *2*, organic-mineral silt (silty gyttja); *3*, terrigenous–carbonate lacustrine silt with an admixture of organic matter; *4*, terrigenous–carbonate lacustrine silt; *5*, sandy organic-mineral silt (sandy gyttja); *6*, peaty gyttja; *7*, sandy loam with admixture of organic matter; *8*, sandy loam; *9*, dense gray loam; *10*, erosion contact; *11*, mollusk shells; *12*, shell detritus. Granulometric fractions (μm): *13*, <1; *14*, 1–5; *15*, 5–10; *16*, 10–50; *17*, 50–100; *18*, 100–250; *19*, 250–500; *20*, 500–1000.

silt (bed 3). In the coastal zone, thin layer 2 is often underlain by sands.

The contact between layers 2 and 3 is usually well-defined, indicating erosion, which is confirmed by the dating (Fig. 2). Thus, according to the age model, the W-2006 core [14] at 90.7 m asl has a hiatus between 3.7 and 2.4 cal ka B.P. A break in the NER-3 core, recorded at 89.6 m asl, is estimated on the basis of a correlation as 6.3 to 5.2 cal ka B.P.

Layer 3 is characterized by a high content of carbonates (61–77%) and an admixture of organic matter up to 15%. The thickness of layer 3 varies from 2.0 m at the middle depths to 4.4 m at the trough bottom (NER-5). The age of formation of layer 3 according to the most complete NER-5 core is estimated within the boundaries of 9.2 to 6.5 cal ka B.P. The grain size composition of layer 3 shows a high sand content, especially in the NER-5 core, from 10 to 45%. The clay content varies from 5 to 37%. The layer with a high clay content within layer 3 is clearly defined in the NER-3 and NER-5 cores. This clay layer, together with the typical shape of magnetic susceptibility variations and LOI, can be considered as a marker horizon. It is also distinguished in the W-2006 core. According to the age model on the basis of the NER-5 core, the time of formation of this marker horizon is estimated at 7.2–7.5 cal ka B.P. The fine-grained composition of the sediment suggests calm and relatively deep conditions of sedimentation, distant from shores and river mouths. The transition to the underlying layer 4 is gradual in the NER-5 core. The NER-3 core shows signs of erosion at the contact between layer 3 and layer 4. In the W-2006 core at the level of 88.7 m asl, the erosion contact of layer 3 with the underlying sandy gyttja of layer 5. The extent of the hiatus, according to age modeling, is 13.0–7.8 cal kal B.P.

Layer 4 is represented by gray terrigenous–carbonate silt with a very high carbonate content (70–83%) and a low organic content (4–6%). Its thickness varies from 1.3 m in the NER-3 core to 3.7 m (visible) in the NER-5 core. In the composition of the silicate part of the sediment, the sand content decreases to 3–10% and the clay content increases significantly to 15–45%. The magnetic susceptibility grows smoothly downwards from the layer top, from 0.1 to 0.23×10^{-3} SI. The NER-3 core at the base of layer 4 shows the erosional contact with the underlying sandy loam of layer 8. The age of the base of layer 4 in this core is estimated at about 10.0 cal ka B.P. on the basis of the correlation with the NER-5 core.

In the bottom areas with middle depths of 1.2–1.8 m, the thin (0.2–0.6 m) member of sandy loams with shell and plant detritus, sometimes with sandy gyttja in the top lies under the terrigenous–carbonate silt everywhere. There are distinct erosional contacts between this member (layers 5–8) and the overlying and underlying layers. Based on the dates from the W-2006 core [14], we can conclude that the formation of this member belongs to the interval 14.7–12.9 cal ka B.P., which coincides with the Late Glacial Interstadial (Bølling–

Allerød Interstadial). The top of this member is established in the range from 85.7 (NER-2) to 88.7 (W-2006) m asl. This member is underlain by dense gray loams with a low content of carbonates (14–20%) and organic matter (3–5%).

Surveys were conducted on Rozhdestvenskii Island, the surface height of which varies from 94.2 to 94.5 m asl. The surface sediments are composed of sands and mineral loams, reworked by the Holocene hydromorphic soil formation. No sediments similar to the Holocene silts of Nero Lake were found.

DISCUSSION

The results allow us to suggest the correlation scheme for three reference columns (Fig. 2), W-2006 [14], NER-3, and NER-5. The diagram clearly demonstrates that the sediment structure at the bottom of the trough is completely different from that of the mid-depth sections. In the trough (NER-5), the upper layer of dark gray organo-mineral silt is almost absent. The erodibility of the upper part of the bottom sediment in the trough is clearly readable on the radargram. The scheme (Fig. 2) shows that, in the Middle Holocene, this trough was significantly less manifested in the bottom relief. It is likely that the modern relief of the trough largely resulted from erosion of the top of the Late Holocene sediment. The nature of this erosion is not completely clear. We suggest two possible mechanisms: (1) the result of sapropel mining in the middle of the 20th century [8]; (2) Late Holocene erosion, caused by increased velocities of the current in the axial part of the lake narrowing. In the NER-5 core, the thickest, most complete, and most conserved sedimentary sequence occurs below the erosion surface. The absence of hiatuses is confirmed by a smooth (step-free) age model. We uncovered Early Holocene terrigenous–carbonate fine-grained silts in the lower part of the NER-5 core, proving the existence of a lake reservoir in the deepest part of the lake basin at that time.

Stratigraphic unconformities have been recorded in the structure of lacustrine sediments at middle depths (1.2–1.8 m). For the NER-3 and W-2006 cores, the following hiatuses and absolute elevations of the erosional contacts were established: <10. 0 cal ka B.P. (86.4 m asl), 13.0–7.8 cal ka B.P. (88.7 m asl), 6.3–5.2 cal ka B.P. (89.6 m asl), and 3.7–2.4 cal ka B.P. (90.7 m asl). These hiatuses allow us to estimate the maximum water levels in the lake at the respective stages (Fig. 3). In reconstructing these levels, we have added 1 m to the height of the erosion boundaries, taking into consideration the possibility of wave erosion of the bottom sediment in shallow water. The upper limit of the mean annual level beyond the stages mentioned was estimated on the basis of the results of the Rozhdestvenskii Island survey, where no Holocene lacustrine sediments were recorded in the structure of the surface cover. The minimum possible level was estimated on the basis of the age modeling data. The age and elevations of all lacustrine sediments, taken with a discreteness of 1 cm, formed a curve, below which the lake level could not drop (Fig. 3).

The established large hiatuses in sedimentation and the referencing sandy loam layers at the base of the carbonate–terrigenous silt indicate the presence of the regressive stage in the history of the lake in the interval from 14.7–10 cal ka B.P. The beginning of the regression (14.7–14.4 cal ka B.P.) was accompanied by a dramatical increase in sand input into the lake, which may indicate an increase in water discharge into rivers. Our estimates show that, during the regression, the lake level dropped below 87 m asl. This is almost 7 m below the mean annual level (93.5 m) [3], which was established for the middle of the 20th century, i.e., before the construction of dam on the Veksa River in the late 1980s. During the regression, the lake was reduced by several times, the water body was preserved only in the axial deepest part of the basin.

The deep Early Holocene regression was followed by a rather rapid growth of the lake level at the end of the Boreal period. At the beginning and middle of the Atlantic period (9.0–6.5 cal ka B.P.), the lake level could have reached 91–94 m asl, which corresponds to the modern parameters. The established transgression is generally consistent with the results of the diatom analysis [5], which showed a high content of planktonic species in the first half of the Atlantic period, indicating relatively deep-water conditions at that time.

Starting from 6.5 cal ka B.P., the lake level decreases rather rapidly, eutrophication grows, and the content of organic matter in sediments increases significantly. At the lowest point of the regressive phase, the level did not exceed 90.6 m. About 5.2 cal ka B.P., the water level starts slowly recovering, but does not reach the present-day levels. The regressive stage of the Late Atlantic–Early Subboreal is confirmed by finds of cultural layers and soils below the modern lake level in the sections of low terraces [1]. On the middle of the already low level at the beginning of the Sub-Atlantic, short-term shoaling to a level of about 91.7 m was recorded. From 2.4 cal ka B.P., the lake level slowly increases, reaching the present-day (before construction of the dam) levels about 300–500 years ago.

Considering the flow-through type of Nero Lake during the entire Holocene and the absence of a significant underground flow, the mandatory condition for a significant drop in the water level should be the decrease in the height of the flow threshold, i.e., erosion in the channel of an outflowing river (the Veksa River). However, deepening of the Veksa River channel under the conditions of extremely low gradients of the Ustya and Kotorosl rivers is not possible without downcutting of the latter. At present, the Ustya–Kotorosl channel [10] at the site of the Veksa River

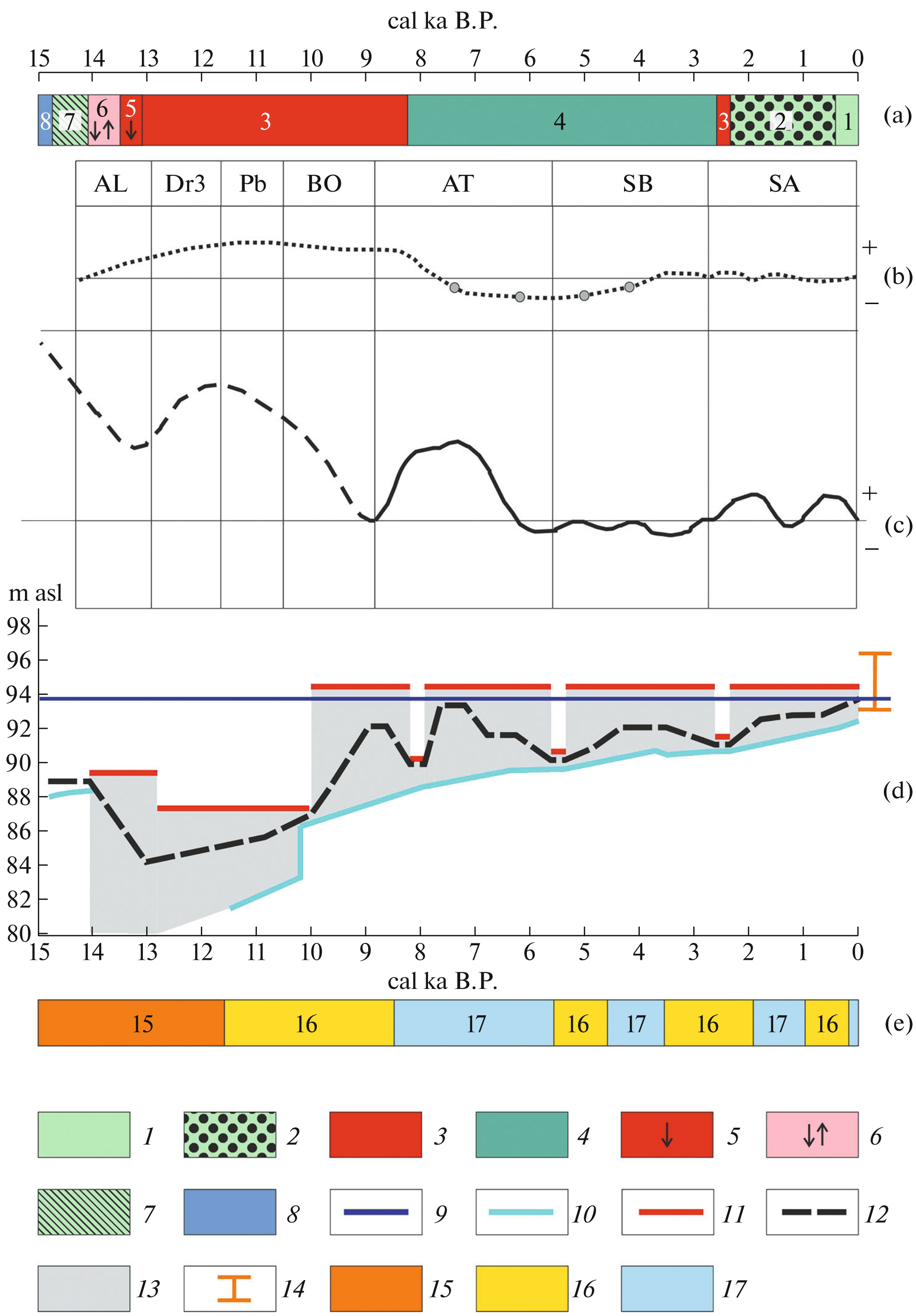

Fig. 3. Changes in the level of Nero Lake in the Holocene, comparison of the results of different authors. Letter designations: a, according to [14]; b, according [1]; c, according to [5]; d, author's version; e, change in fluvial activity in the center of the East European Plain [12]. Legend: *1*, shallow eutrophic lake; *2*, shallow oxygen-free lake with high acidity; *3*, hiatus in sedimentation (level drop); *4*, shallow lake; *5*, possible shoaling of the lake/coast line; *6*, level fluctuations and gradual shoaling; *7*, shallow eutrophic/mesotrophic lake; *8*, shallow oligotrophic lake; *9*, mean annual level according to data for the middle of the 20th century [3]; *10*, the minimum probable mean annual level; *11*, the maximum probable mean annual level; *12*, author's estimation of the mean annual level change; *13*, probable field of the mean annual level fluctuation; *14*, recorded amplitude of level fluctuations during 1930s–1980s [3]; *15*, epoch of extreme high river runoff; *16*, high fluvial activity; *17*, low fluvial activity.

mouth is in the regime of intensive accumulation and level growth. This is indicated by active meandering and a leveed character of channels. Before the construction of the dam in Belogostitsy, even reverse gradients on the Veksa River [3] were noted during major floods on the Ustya—Kotorosl system, which led to countercurrent and flooding on Nero Lake. All this indicates the direct dependence of the Nero Lake level on the erosion and accumulative regime in the Ustya–Kotorosl river system.

Comparison of the level fluctuation curve of Nero Lake (Fig. 3d) with the fluvial intensity diagram (Fig. 3e) reveals a significant relationship. It is likely that the large regression of the lake in the Late Glacial and Early Holocene was caused by the extremely high discharges and the deep downcutting of river channels [12, 13]. The consequence of this was a significant drop in the height of the runoff threshold and the actual transformation of Nero Lake into a small lake-like extension at the confluence of the Sara and Ishnya rivers. The transgression of Nero Lake in the Atlantic period coincides with the minimum level of fluvial activity in the Holocene, which created the preconditions for intensive accumulation in the Ustya–Kotorosl valley. Subsequent small regressions generally coincide in time with the growth of fluvial activity.

CONCLUSIONS

(1) The deep regression of the level of Nero Lake in the Late Glacial and Early Holocene was established. Stratigraphic unconformities in the sediments point to the stage of the low-level position (below 87 m asl) between 14.7 and 10.0 ka B.P. The lake decreased in size several times; the water body was preserved only in the axial deepest part of the basin.

(2) The large transgressive phase was recorded at the beginning and in the middle of the Atlantic period from 9.0 to 6.5 ka B.P. The lake level reached 91–94 m asl, which is close to the current values. The mean annual level did not rise above the 94.2 m asl in the Holocene.

(3) In the interval 6.5–2.4 ka B.P., the regressive position of the mean annual level was reconstructed; it is lower than the modern one by about 1–3 m.

(4) From 2.4 ka B.P., the level of Nero Lake grew slowly, reaching modern levels about 300–500 years ago.

(5) The main factor of Nero Lake level fluctuations in the Holocene was transformation of channel systems that caused changes in the height of the runoff threshold of the lake.

This transformation was caused by both the climatic changes in fluvial activity and the internal self-development of river channels.

FUNDING

The laboratory and analytical studies and the reconstruction of fluctuations in the level of Nero Lake were supported by a Mega-grant (Agreement no. 075-15-2021-599, June 8, 2021). Field work was supported by a grant of the Russian Science Foundation, project no. 18-77-00083.

CONFLICT OF INTEREST

The authors declare that they have no conflicts of interest.

REFERENCES

1. A. L. Aleksandrovskii, Eurasian Soil Sci. **44** (10), 1055–1068 (2011).
2. A. A. Barysheva, Extended Abstract of Candidate's Dissertation in Geography (Mosk. Obl. Ped. Inst., Moscow, 1953).
3. E. S. Bikbulatov, E. M. Bikbulatova, A. S. Litvinov, and S. A. Poddubnyi, *Nero Lake: Hydrology and Hydrochemistry* (Rybinskii dom pechati, Rybinsk, 2003) [in Russian].
4. V. S. Gunova, Extended Abstract of Candidate's Dissertation in Geography (Mosk. Gos. Univ., Moscow, 1975).
5. V. S. Gunova and O. N. Leflat, Vestn. Mosk. Univ., Ser. 5: Geogr., No. 4, 42–45 (1997).
6. D. D. Kvasov, *The Late Quaternary History of Large Lakes and Inland Seas of Eastern Europe* (Nauka, Leningrad, 1975) [in Russian].
7. Yu. A. Lavrushin, E. A. Spiridonova, and A. V. Engovatova, Stratigr. Geol. Correl. **24** (6), 637 (2016).
8. A. V. Smirnov, Tr. Lab. Sapropelevykh Otlozh., No. 6, 201–213 (1956).
9. N. G. Sudakova, V. V. Dashevskii, V. V. Pisareva, et al., in *27th Int. Geol. Congr. Excursion Guide* (Moscow, 1984) [in Russian].
10. N. V. Chizhikov, Tr. Lab. Sapropelevykh Otlozh., No. 6, 130–144 (1956).
11. W. E. Dean, J. Sedimentary Res. **44** (1), 242–248 (1974).
12. A. Panin and E. Matlakhova, Catena, No. 130, 46–61 (2015).
13. V. Ukraintsev, E. Konstantinov, and A. Zakharov, Limnol. Freshwater Biol. **4** (1), 476–477 (2020).
14. B. Wohlfarth, P. Tarasov, O. Bennike, T. Lacourse, D. Subetto, P. Torssander, and F. Romanenko, J. Paleolimnol. **35** (3), 543–569 (2006).

Translated by V. Krutikova